Reviving recovered carbon black as reinforcement for natural rubber by utilizing acylhydrazine-functionalized polysulfide as an intelligent interfacial modifier

Senmao Yu,[a] Zhenghai Tang,*[a] Dong Wang,[a] Siwu Wu,[a] Fei Chen,[b] Baochun Guo*[a] and Liqun Zhang[ab]

[a] Institute of Emergent Elastomers, Guangdong Basic Research Center of Excellence for Energy & Information Polymer Materials, School of Materials Science and Engineering, South China University of Technology, Guangzhou 510640, China

[b] School of Chemical Engineering and Technology, Xi'An JiaoTong University, Xi'an 710049, China

*Corresponding authors: mszhtang@scut.edu.cn (Z. Tang); psbcguo@scut.edu.cn (B. Guo).

Characterization

X-ray diffraction (XRD) patterns were acquired using an X'pert Powder instrument. Fourier-transform infrared (FTIR) tests were conducted on a Thermo Fisher Scientific Nicolet IS50 spectrometer. Differential scanning calorimetry (DSC) tests were performed on a TA DSC 25 differential scanning calorimeter. To determine the thermal properties, samples were heated from -60 to 150 °C at 3 °C/min; to measure the freezing point of cyclohexane, swollen composites were cooled from 25 to -25 °C at 3 °C/min. Matrix-assisted laser desorption/ionization time-of-flight mass spectrometry (MALDI-TOF-MS) test was performed on Bruker autoflex III smartbean. Thermogravimetric curves were acquired using a TA Q50 thermogravimetric analyzer (TGA) with a heating rate of 10 °C/min under nitrogen atmosphere. Raman spectra were measured using an HJY LabRAM Aramis spectrometer equipped with a He-Ne laser. ^{1}H nuclear magnetic resonance

(NMR) tests were conducted on a Bruker AVANCE III HD 600 instrument. X-ray photoelectron spectra (XPS) were performed on an Escalab Xi^+ instrument with an Al Kα radiation source and the results were fitted using Avantage software. Elemental analysis tests were carried out on an Elemental Vario EL cube instrument.

Rheological properties of uncured compounds and vulcanizates were determined on an Alpha RPA 2000 rubber processing analyzer (RPA). Transmission electron microscopy (TEM) images were captured using a JEM-2100F instrument. Scanning electron microscopy (SEM) images of the cryogenically fractured surface of composites were shot by a Hitachi S-4800 instrument.

Bound rubber (BR) content of uncured compounds and swelling ratio of vulcanizates were measured based on equilibrium swelling experiments, as described elsewhere [1]. Uniaxial tensile experiments were conducted on a Shimadzu AGX-V instrument at room temperature with an extension rate of 500 mm/min. The specimens were dumbbell shaped with an effective gauge length of 40 mm, a width of 4 mm and a thickness of approximately 0.4 mm. Compression fatigue heat built-up of the composites was tested using a U-CAN UD-3801 flexometer at 55 °C with the frequency of 30 Hz and preload of 1 MPa. Rolling resistance of the composite wheels was determined using an RSS-II type rolling resistance tester, with a load of 30 kg and a rotation speed of 1200 r/min.

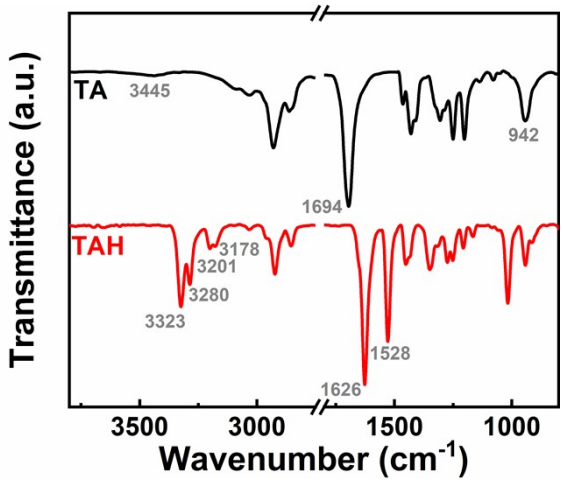

Fig. S1 FTIR spectra of TA and TAH.

TAH was synthesized through the amidation reaction of TA with hydrazine monohydrate. In the FTIR spectrum of TA, the absorptions at 3445 and 1694 cm^{-1} are attributed to the stretching vibrations of -OH and C=O in the carboxyl group, respectively; and the absorption at 942 cm^{-1} is ascribed to the bending vibration of the carboxylic acid dimers.[1] In the FTIR spectrum of TAH, the aforementioned absorptions associated with the carboxyl group of TA are disappeared. In addition, several new absorptions related to the acylhydrazine group are accordingly observed. Specifically, the absorptions at 3323 and 3280 cm^{-1} along with 3201 and 3178 cm^{-1} correspond to the stretching vibrations of -NH and $-NH_2$, respectively; [2] and the absorptions at 1626 and 1528 cm^{-1} are ascribed to amide I and II bands, respectively, indicating the occurrence of amidation reaction.[3] These results confirm that the carboxyl group in TA is successfully converted to acylhydrazine group.

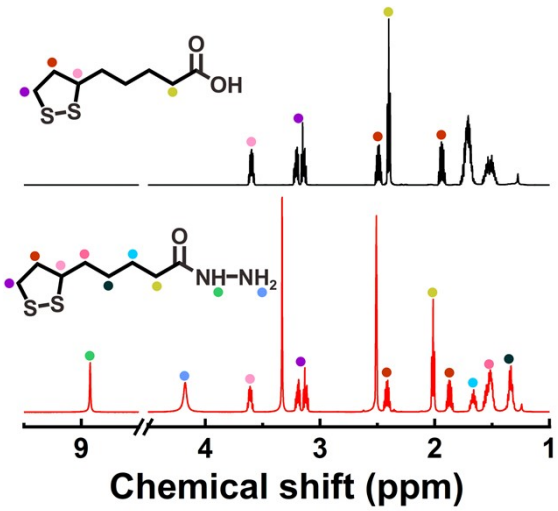

Fig. S2 ^{1}H NMR spectra of TA and TAH.

In the ^{1}H NMR spectrum of TA, the resonance signals at 3.58 and 3.14 ppm are attributed to the protons on the tertiary and secondary carbon adjacent to sulfur atom in the five-membered ring, respectively; the resonance signals at 2.50 and 1.92 ppm are ascribed to the protons on -CH_2 next to the tertiary carbon in the ring; and the resonance signal at 2.41 ppm corresponds to the protons on -CH_2 adjacent to the carbonyl group.[4] In the ^{1}H NMR spectrum of TAH, new resonance signals are emerged at 8.93 and 4.16 ppm, which are associated with the protons on -NH and -NH_2, respectively. In addition, upon amidation reaction, the resonance signal related to the protons on -CH_2 adjacent to carbonyl group shifts from 2.41 to 2.01 ppm.[2]

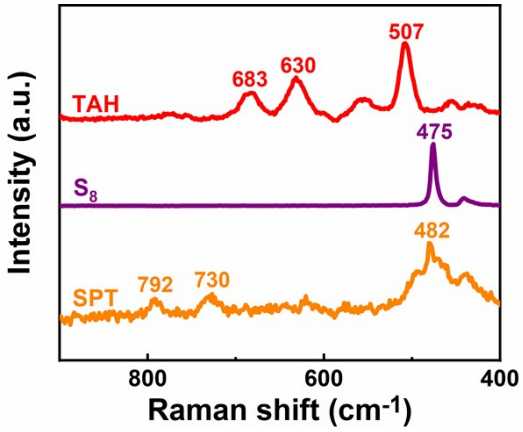

Fig. S3 Raman spectra of TAH, S_8 and SPT.

In the Raman spectrum of TAH, the absorptions at 683 and 630 cm^{-1} along with 507 cm^{-1} correspond to the stretching vibrations of C-S and S-S, respectively. In the Raman spectrum of S_8, the absorption at 475 cm^{-1} is due to the stretching vibrations of S-S. For SPT, the absorptions at 792 and 730 cm^{-1} are attributed to the stretching vibrations of C-S_n, and the absorption at 480 cm^{-1} is due to the stretching vibrations of polysulfide bonds, respectively. These outcomes indicates that TAH undergoes ring-opening copolymerization with S_8.[5]

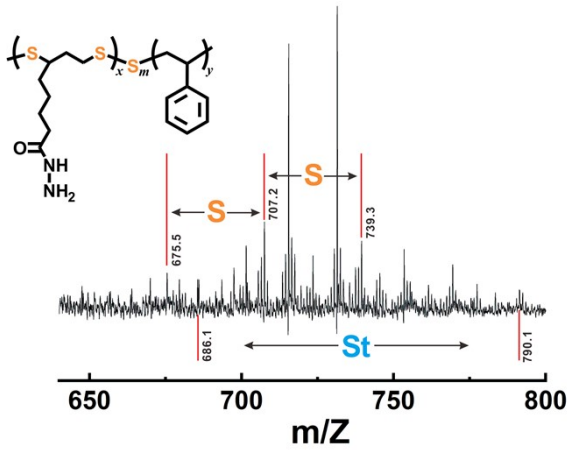

Fig. S4 MALDI-TOF-MS spectrometry of SPT using THF as solvent.

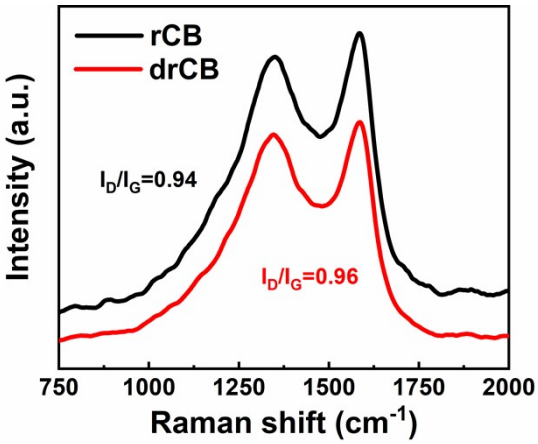

Fig. S5 Raman spectra of rCB and drCB.

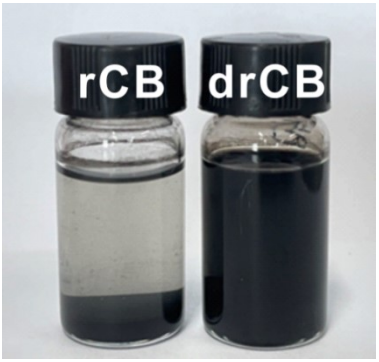

Fig. S6 Photographs of rCB and drCB suspended in water (0.6 mg/mL) after settling for 2 weeks.

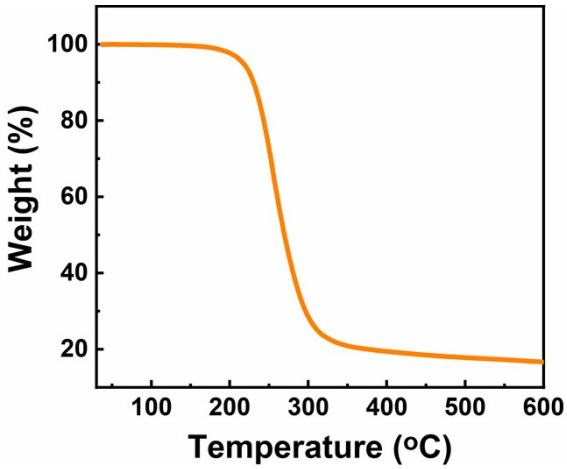

Fig. S7 TGA curve of SPT.

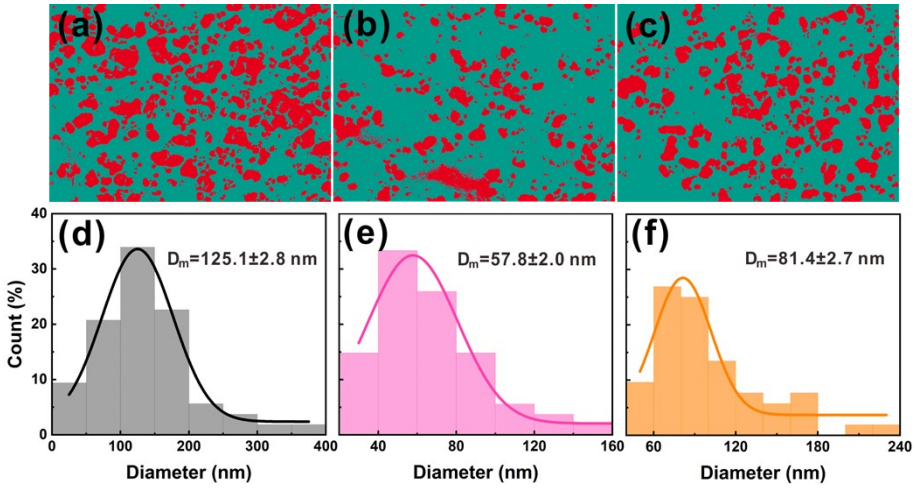

Fig. S8 Images used for the quantitative analysis of drCB agglomerates in (a) NR/SPT-0, (b) NR/SPT-0.5 and (c) NR/SPT-0.7 composites by Image-J software; the size distribution of drCB agglomerates in (d) NR/SPT-0, (e) NR/SPT-0.5 and (f) NR/SPT-0.7 composites.

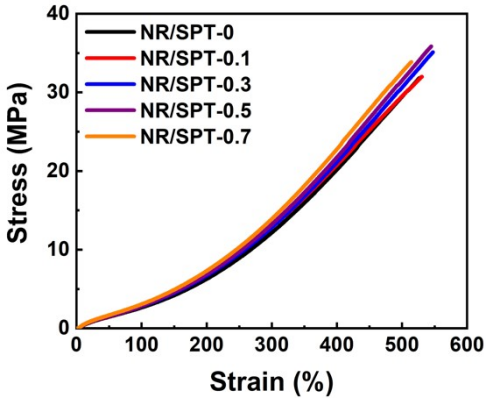

Fig. S9 Typical stress-strain curves of NR/SPT-*x* composites.

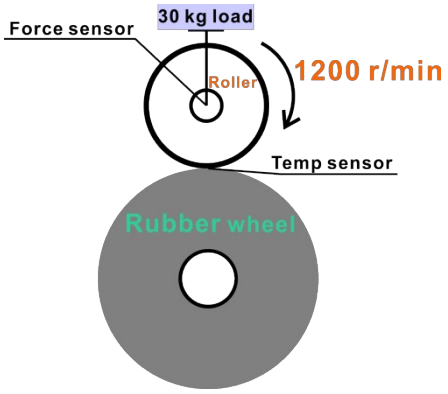

Fig. S10 Schematic diagram of the RSS-II type rolling resistance tester.

References

1 S. Yu, Z. Tang, S. Wu and B. Guo, Use of naturally small molecule as an intelligent interfacial modifier for strengthening and toughening silica-filled rubber composite, *Compos. Sci. Technol.*, 2022, **227**, 109624.

2 Y. Deng, Q. Zhang, C. Shi, R. Toyoda, D.H. Qu, H. Tian and B.L. Feringa, Acylhydrazine-based reticular hydrogen bonds enable robust, tough, and dynamic supramolecular materials, *Sci. Adv.*, 2022, **8**, eabk3286.

3 D. Wang, Z. Tang, R. Huang, Y. Duan, S. Wu, B. Guo and L. Zhang, Interface coupling in rubber/carbon black composites toward superior energy-saving capability enabled by amino-functionalized polysulfide, *Chem. Mater.*, 2023, **35**, 764.

4 C.Y. Shi, Q. Zhang, B.S. Wang, M. Chen and D.H. Qu, Intrinsically photopolymerizable dynamic polymers derived from a natural small molecule, *ACS Appl. Mater. Interfaces*, 2021, **13**, 44860.

5 Y. Deng, Z. Huang, B.L. Feringa, H. Tian, Q. Zhang and D.-H. Qu, Converting inorganic sulfur into degradable thermoplastics and adhesives by copolymerization with cyclic disulfides, *Nat. Commun.*, 2024, **15**, 3855.